Supplementary Information

Mitigating effect of organic matter on the *in vivo* toxicity of metal oxide nanoparticles in the marine environment

Seta Noventa*[a], Darren Rowe[a] and Tamara Galloway[a]

*corresponding author: email: s.noventa2@exeter.ac.uk, tel: 01392 263436

[a] College of Life and Environmental Sciences, University of Exeter, EX4 4QD, Exeter UK,

This file includes additional information about:

- Primary physico-chemical properties of the test-NPs and methods used for the characterization
- Methods for the characterization of the behaviour of the test-NPs
- Primer sequences, qPCR conditions and performance
- MnO_2 NP aggregation kinetics
- MnO_2 NP ingestion
- TEM-EDS study of cellular internalization of MnO_2 NPs
- TEM-EDS analyses of electron dense particles suspected of being cellular internalized BSA coated MnO_2 NPs

Abbreviations: NPs: nanoparticles; TEM: Transmission Electron Microscopy; BET: Branauer, Emmett and Teller; SEM: Scanning Electron Microscope; EDS: Energy Dispersive X-ray Spectroscopy; $pH_{IEP:}$ pH at the isoelectric point; DIW: deionised water; ASW: artificial seawater; Cyt c: Cytochrome c.

Primary physico-chemical properties of the test-NPs and methods used for the characterization

The primary physico-chemical proprieties of the test NPs, ZnO NPs, and MnO_2 NPs, are summarized in Table S1. Data was retrieved from official reports (for ZnO NPs only [1]) and supplemented with data performed at the NERC Facility for Environmental Nanoscience Analysis and Characterisation (FENAC, Birmingham, UK). The description of the methods used and more details about the results obtained are reported below.

Table S1. Primary physico-chemical proprieties of the test NPs, ZnO NPs and MnO_2 NPs. Data reported in italics were obtained from the characterization programme carried out at the NERC Environmental Nanoscience Facility (FENAC, Birmingham, UK); those reported in regular font were retrieved from the official reports and the literature.

	ZnO NPs	**MnO_2 NPs**
CODE, SUPPLIER	NM112, OECD's sponsorship programme for the global safety assessment of nanomaterials (www.nanotechia.org)	4910DX, Skyspring Nanomaterials INC, Houston, USA
DESCRIPTION		*MnO_2*
SHAPE (TEM)	Near spherical rather than polyhedral with regular morphology and a relatively homogenous size distribution. Generally, particles have an aspect ratio close to 1 [1]	*Almost tetragonal, but with a quite variable aspect ratio. Based on the aspect ratio distribution, three groups can be distinguished: group 1 (85% of total particles): 1.9 ± 0.6 (as mean aspect ratio); group 2 (7% of total particles): 4.7 ± 0.5; group 3 (7% of total particles): 7.6 ± 0.6.*
PRIMARY PARTICLE OR CRYSTAL SIZE (TEM)	20-50 nm [1]	*The longest and the smallest size of each particle are highly variable. For the three aspect ratio based groups they are (longest size x smallest size, as average): 27x15nm (group 1), 62x13 nm (group 2), 75x10 nm (group 3).*
SPECIFIC SURFACE AREA (BET)	27.2 ± 1.2 $m^2 g^{-1}$ [1]	*34.5 $m^2 g^{-1}$*
PURITY (SEM-EDS)		*Purity (Mn-O): 94.7%. Mn (58.62%), O (36.13%), F (4.33%), Na (0.35%), Si (0.02%), S (0.44%), K (0.01%), Fe (0.06%), Cu (0.04%).*
pH_{IEP} (ELECTROKINETIC METHOD)	*10.4*	*4.8*

CRYSTALLITE PHASE (XRD): STRUCTURE AND DIAMETER	Hexagonal zincite. Diameter: 24.1 nm [1]	*Akhtenskite, synthetic. Crystal system: hexagonal; Space group: P63/mmc (194); Unit cell parameters: a (Å) 2.786 nm; b (Å) 2.786 nm; c (Å) 4.412 nm α(°)=90; β(°)=90; γ(°)=120*

Primary structure (TEM)

TEM-samples were prepared by drop deposition: 30 µL of the sample was deposited onto the carbon film supported by a 200 mesh copper TEM-grid (Agar Scientific). The grids were covered and left to stand for 1 hr, and the drop of sample was topped up to prevent drying, if required. The residual liquid was wicked onto absorbent paper, and the TEM-grids were washed four times by immersion in separate 25mL tubes of DIW for 30 secs, and dried overnight. Sizes and shapes of NPs were characterized on a JEOL 1200EX TEM, using 80 keV electron generation. Images were acquired at 30,000, 50,000 and 100,000 times magnification. Figure S1 shows a representative TEM image of on MnO_2 NPs under pristine conditions.

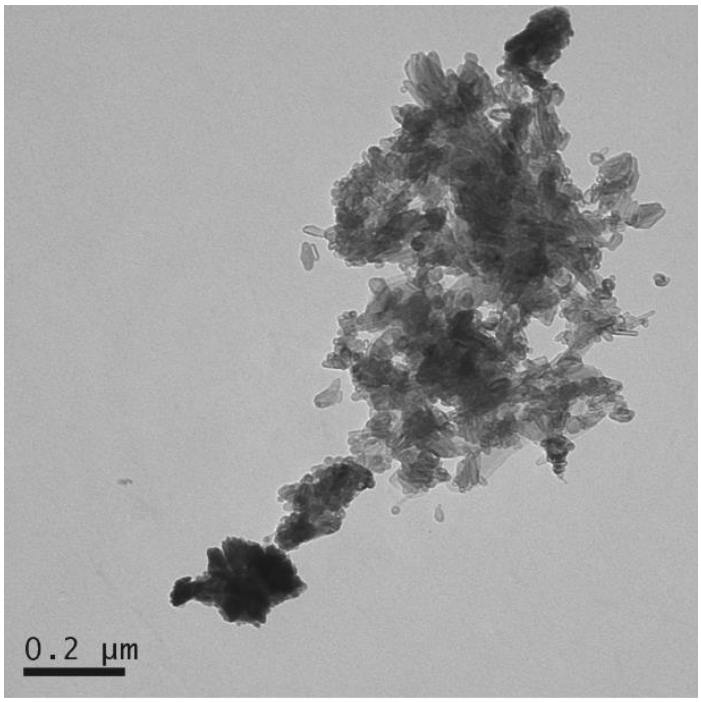

Figure S1. TEM image of the test MnO_2 NPs.

Surface area (BET)

Surface area measurements were carried out using a Beckman Coulter SA31000 Surface Area Analyser (BET). Duplicate measurements were carried out on the nanomaterial. The weights of clean, dry sample tubes were recorded, and the nanomaterial was introduced into the tubes. The tubes were fitted into the BET ports for drying the sample, and the material was dried at 150°C for 180 mins under flowing helium gas, and the tube cooled to room temperature.

The dried samples and tubes were weighed, and the dry sample weights were calculated. The first tube was installed in the measurement port of the BET and the bulb of the tube containing the sample was immersed in liquid N_2. The tube was evacuated, then helium gas, containing different partial pressures of nitrogen was introduced into the tube. The nitrogen was adsorbed onto the surface of the powder and the instrument calculated the surface area of the powder from the drop in pressure. The measurement was repeated for the second tube.

pH_{IEP} (electrokinetic method)

The pH_{IEP} of the three test-NPs was determined via electrokinetic method (i.e. measurements of the zeta potential as a function of pH). The electrophoretic mobility measurements were performed through a Zetasizer Nano ZS (Malvern Instruments Ltd. Malvern, UK) operating with a He-Ne laser at a wavelength of 633 nm using back scattered light. The zeta potential values were computed through the application of the Smoluchowsky approximation.

Zeta potential was measured over a set of 200 µM NPs dispersions in 10 mM NaCl (samples' conductivity: 1.2 ± 0.1 mS cm^{-1}) at different pH. The pH was decrease-increase by the addition of proper volumes of NaOH or HCl (0.1M). Replicated measurements were taken at 25°C in General Purpose mode. The applied voltage was 150V and the number of runs for each measurement was selected automatically (12 at least). The pH_{IEP} values reported in Table S1 were obtained from the data presented in Figure S2. The graph plots the average values of six replicated measurements of zeta potential versus the pH featuring the NPs suspensions.

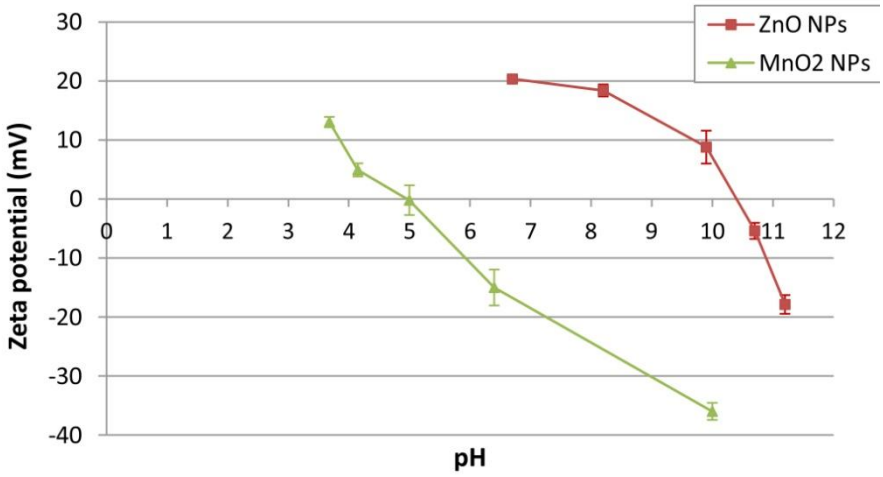

Figure S2. Zeta potential of the test-NPs, dispersed in 10 mM NaCl, as a function of pH. Mean and standard deviation of 6 replicated measurements of zeta potential versus pH.

Crystal structure (XRD)

The crystalline structure of test Mn oxide nanopowder (Skyspring Nanomaterials Inc, Houston, USA; 4910DX) was determined by Powder X–ray (XRD) diffraction. Powder x-ray diffraction was carried out on a Bruker D8 Advance, using copper Kα radiation, at a wavelength of 1.5406 Å, and on a Bruker D2, using cobalt Kα radiation at a wavelength of 1.788965 Å. Measurements were carried out at room temperature with a step size of 0.02 degrees 2θ and 10 second dwell time.

Contrary to the claim of the manufacturer, who sold the material as Mn_2O_3, the manganese oxide nanopowder (Skyspring Nanomaterials Inc, Houston, USA; 4910DX) was identified as $Mn(IV)O_2$. The automatic match was obtained with Akhtenskite synthetic (ICDD card 01-089-5171; Figure S3A), which appeared to be the main form present and gave a good match for most peaks in both the position and the relative heights. Additionally, good correspondence with reflections from Ramsdellite, another $Mn(IV)O_2$ phase, was obtained for some of the peaks. Nsutite, a mixed state oxide which is predominantly Mn^{4+} (typically $Mn^{4+}_{0.94}\ Mn^{2+}_{0.06}O_{1.88}(OH)_{0.12}$), was also identified as a possible match for some peaks (Figure S3A). In contrast, the presence of Mn^{3+} oxide phases (*i.e.* Mn_2O_3, Mn_3O_4) was excluded by the lack of match with the reference patterns of Bixbyite-C syn (Mn_2O_3, ICDD card 00-041-1442) and Hausmannite (Mn_3O_4, ICDD card 00-024-0734, 01-080-0382; Figure S3B). The lattice parameters and crystalline structure of Akhtenskite syn are summarized in Table S2.

The mineral Akhtenskite (also known as ε-MnO_2) is a polymorph of pyrolusite (β-MnO_2, tetragonal structure, 1x1 tunnels) and Ramsdellite (orthorombic structure, 2x1 tunnels). Akhtenskite has an electrochemical activity similar to that of γ-MnO_2 (i.e. an intergrowth of pyrolusite in a ramsdellite phase with varying degrees of microtwinning, which is widely used in MnO_2/Zn couple of alkaline primary batteries[2]). The structure of these MnO_2 polymorphs consists of [MnO_6] octahedra with different arrangements of edge and corner sharing. According to the electrochemists community, the presence of tunnels in the crystal structure of these materials, in particular 2 x 1 tunnels, explain their high electrochemical activity [2]. For a more detailed description of ε-MnO_2 refer to[2].

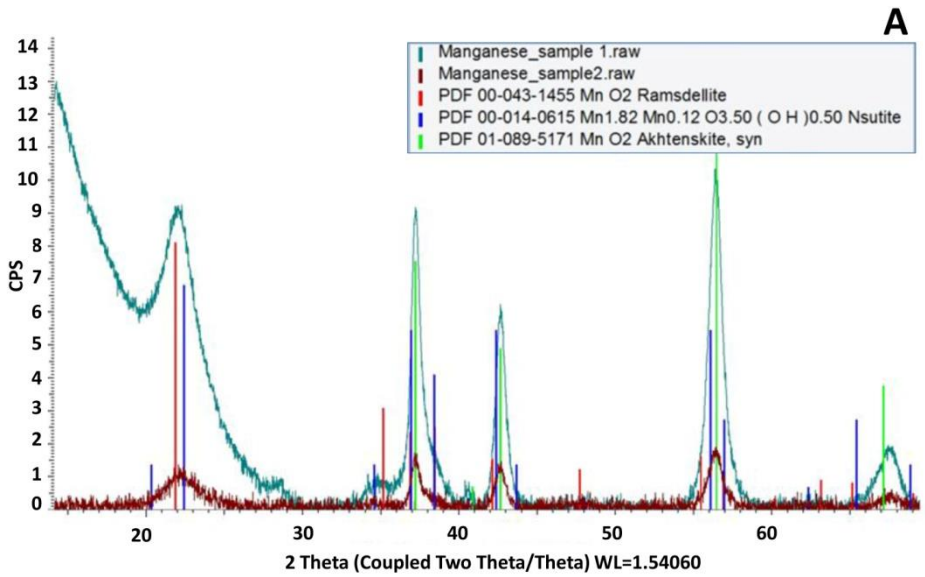

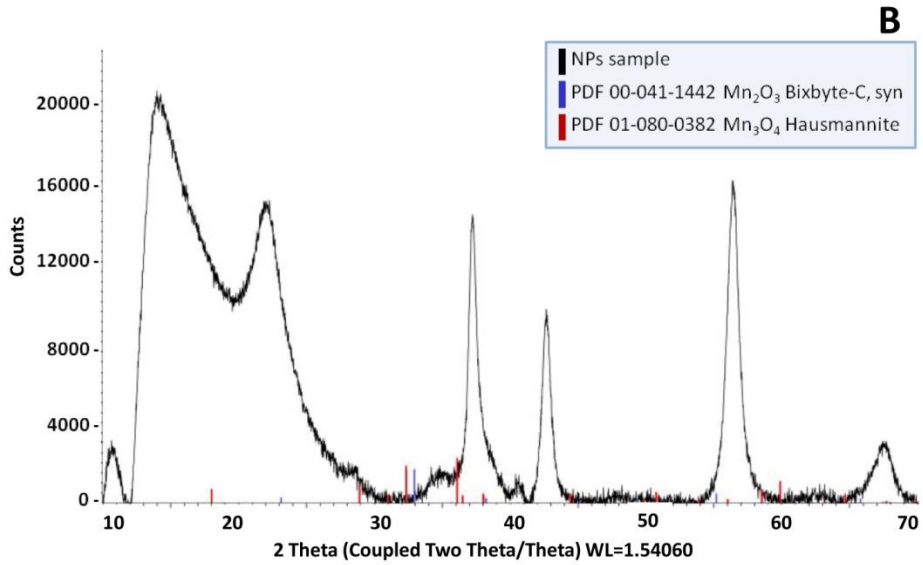

Figure S3. Powder X–ray diffraction (XRD) profiles. A) XRD profiles of Skyspring Nanomaterials 4910DX manganese oxide nanopowder plotted against the peak profiles of Ramsdellite, Nsutite and Akhtenskite syn ($Mn(IV)O_2$). *Manganese_sample 1* profile is the XRD profile obtained through copper Kα radiation, at a wavelength of 1.5406 Å (Bruker D8 Advance); *Manganese_sample 2* profile is the XRD profile obtained through cobalt Kα radiation at a wavelength of 1.788965 Å (Bruker D2). Data of the *Manganese_sample 2* have been re-calculated to provide a direct comparison at the wavelength from the copper source used for the *Manganese_sample 1*. B) Powder X–ray diffraction profile of manganese oxide nanopowder (Cu Kα radiation, 1.540596 Å) plotted against the peak profiles of Mn^{3+} oxides (Bixbyite-C syn, Mn_2O_3; Hausmannite, Mn_3O_4).

Table S2. Lattice parameters and crystalline structure of MnO_2 Akhtenskite synthetic (PDF card 01-089-5171).

Metal oxide NPs	Crystal system	Space group	Unit cell parameters					
			a (Å)	b (Å)	c (Å)	α (°)	β (°)	γ (°)
MnO_2	Hexagonal	P63/mmc (194)	2,786	2,786	4,412	90	90	120

Methods for the characterization of the behaviour of the test NPs

Hydrodynamic size of NPs in seawater

The hydrodynamic diameter of the particles in ASW was determined on a Zetasizer Nano ZS (Malvern Instruments Ltd. Malvern, UK) operating with a He-Ne laser at a wavelength of 633 nm using back scattered light. Samples were held at 20ºC for 2 mins prior to analysis to allow for particle stabilisation. Ten replicate measurements were made on each sample and data are reported as means and the standard deviations of the replicates.

Dissolution

The extent of ZnO NPs dissolution after 24 hrs in ASW and in presence of different concentrations of the model NOM (250 uM suspension; 24°C) was analyzed via ultrafiltration (30 KDa Microsep™ Advance Centrifugal Devices, Pall Life Sciences), followed by microwave assisted acid digestion (2 mL of sample, 1 mL of HNO_3; 1 mL H_2O_2; Ethos EZ, Milestone Inc, Shelton) and elemental analysis (Inductively coupled plasma - mass spectrometry, ICP-MS; Thermo Scientific X Series 2). ASW samples were five-fold diluted with DIW before

undergoing ICP-MS analysis. The ICP-MS instrument was calibrated and operated according to the relevant SOPs contained within the appropriate instrument Record Manual and the instrumental performance checked for conformity with the manufacturer's specifications before the analysis of any samples began. The ICP-MS instrument was tuned and operated in collision/reaction cell mode, with 7% H_2 in He as the reaction/collision gas, to negate the effect of any polyatomic species formed in the plasma or interface region. Any instrumental drift was monitored for by the analysis of check standards every 10 samples. All analyses were conducted under ISO 9001:2008 certification. The instrumental limits of detection (LOD) of Zn was 1.51 ng mL^{-1}. Quantification was performed through calibration curves prepared by purposely diluting a multi-element calibration standard in five-fold diluted ASW.

Sorption

The extent of MnO_2 NPs sorption after 48 hrs weathering in ASW (250 uM suspension; 24°C) was analyzed via ultrafiltration (30 KDa Microsep™ Advance Centrifugal Devices, Pall Life Sciences), followed by microwave assisted acid digestion (2 mL of sample, 1 mL of HNO_3; 1 mL H_2O_2; Ethos EZ, Milestone Inc, Shelton) and elemental analysis (Inductively coupled plasma - mass spectrometry, ICP-MS, Thermo Scientific X Series 2; Inductively Coupled Plasma - Optical Emission Spectrometry, ICP-OES, Thermo Scientific iCAP 7400). ASW samples were five-fold diluted with DIW before undergoing elemental analysis. The concentrations of Cr, Mn, Fe, Co, Ni, Cu, and Cd were analysed by ICP-MS according to the method already described for the dissolution test; the concentrations of Ca, K, Mg, Na, and S were analysed by ICP-OES. The ICP-OES instrument was calibrated and operated according to the relevant SOPs contained within the appropriate instrument Record Manual and the instrumental performance checked for conformity with the manufacturer's specifications before the analysis of any samples began. The emission signal for each element was measured at two different wavelengths (as a check for possible interferences). All analyses were conducted under ISO 9001:2008 certification.

Primer sequences, qPCR conditions and performance

Table S3. qPCR. Primer sequences, qPCR conditions and amplification performance. Housekeeping genes are in italics. Abbreviation: Ta, annealing temperature; E, PCR efficiency; SODmt, mitochondrial superoxide dismutase; AIF-1, allograft inflammatory factor 1; IAPs, inhibitors of apoptosis proteins; MT2, metallothionein 2; EF-1, elongation factor-1; RS18, ribosomal protein S18.

Target gene	Accession number NCBI	Primer direction	Primers' sequences (5'–3')	T_a (°C)	E (%)	References of the primers' sequences
SODmt	EU420128	Sense	ACAAAGTCAATCAGTGCCCT	60	105.9	[3]
		Antisense	CCATTGCCTCTGCCAGT			
AIF-1	JX315461	Sense	ACCACAAACTCTGGCACTATCC	56.7	92.1	[4]
		Antisense	ATGCTGGTATTTCCACTTCCTA			
IAPs	HQ425701	Sense	CATGTTGCCGTGTGGACATC	60	96.4	[5]
		Antisense	ATGCGAGCCAAGTACGGACA			

MT2	AJ297818	Sense	TCCGGATGTGGCTGCAAAGTCAAG	60	97.5	[3]
		Antisense	GGTCCTTTGTTACACGCACTCATTT			
EF-1	AB122066	Sense	CGGAGATGCTGGTATGGTCC	60	103.5	[6]
		Antisense	GTGCAGCCTTGGTGACTTTG			
RS18	AB199895	Sense	GCAGAACCCTCGTCAGTACA	62	97.0	[6]
		Antisense	GTGACGGAGACCTCTGTGTG			

MnO_2 NP aggregation kinetics

In order to assess if the hydrodynamic size (HS) pattern of MnO_2 NPs under the different scenarios was maintained over time (i.e. similar for ASW suspension in absence and in presence on NOM, whereas lower for BSA treated MnO_2 NPs), Dynamic Light Scattering measurements (*DLS;* Zetasizer Nano ZS, Malvern Instruments, UK) were undertaken immediately after the preparation of NP suspensions, and after 2 and 24 h. The test suspensions (200 uM) were manually shaken (10 secs) before undergoing measurement in order to resuspend the settled aggregates. DLS measurements were taken also in DIW to provide reference. The results are plotted in Figure S4.

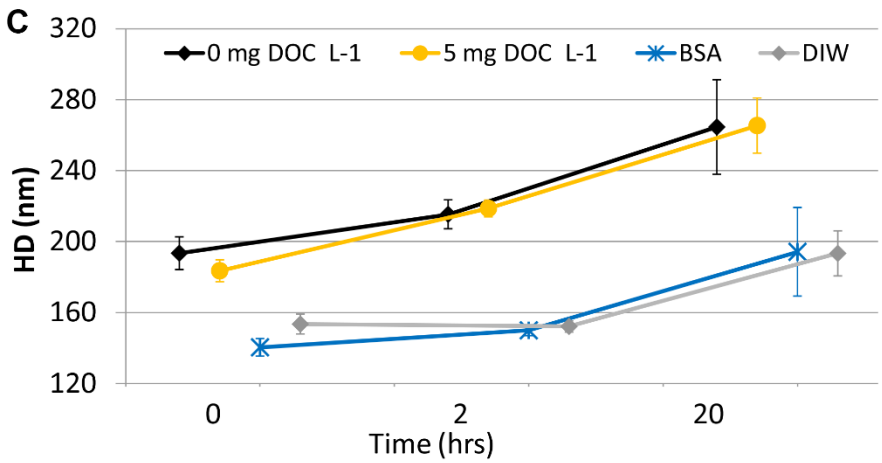

Figure S4. MnO_2 NP aggregation kinetics. Evolution over 20 h of the hydrodynamic size (HD) of MnO2 NPs in 200 uM suspensions in ASW without NOM, with 5 mg DOC L'1, and following BSA pre-treatment.

MnO_2 NP ingestion

Organisms exposed to the treatments containing 50 uM MnO_2 NPs

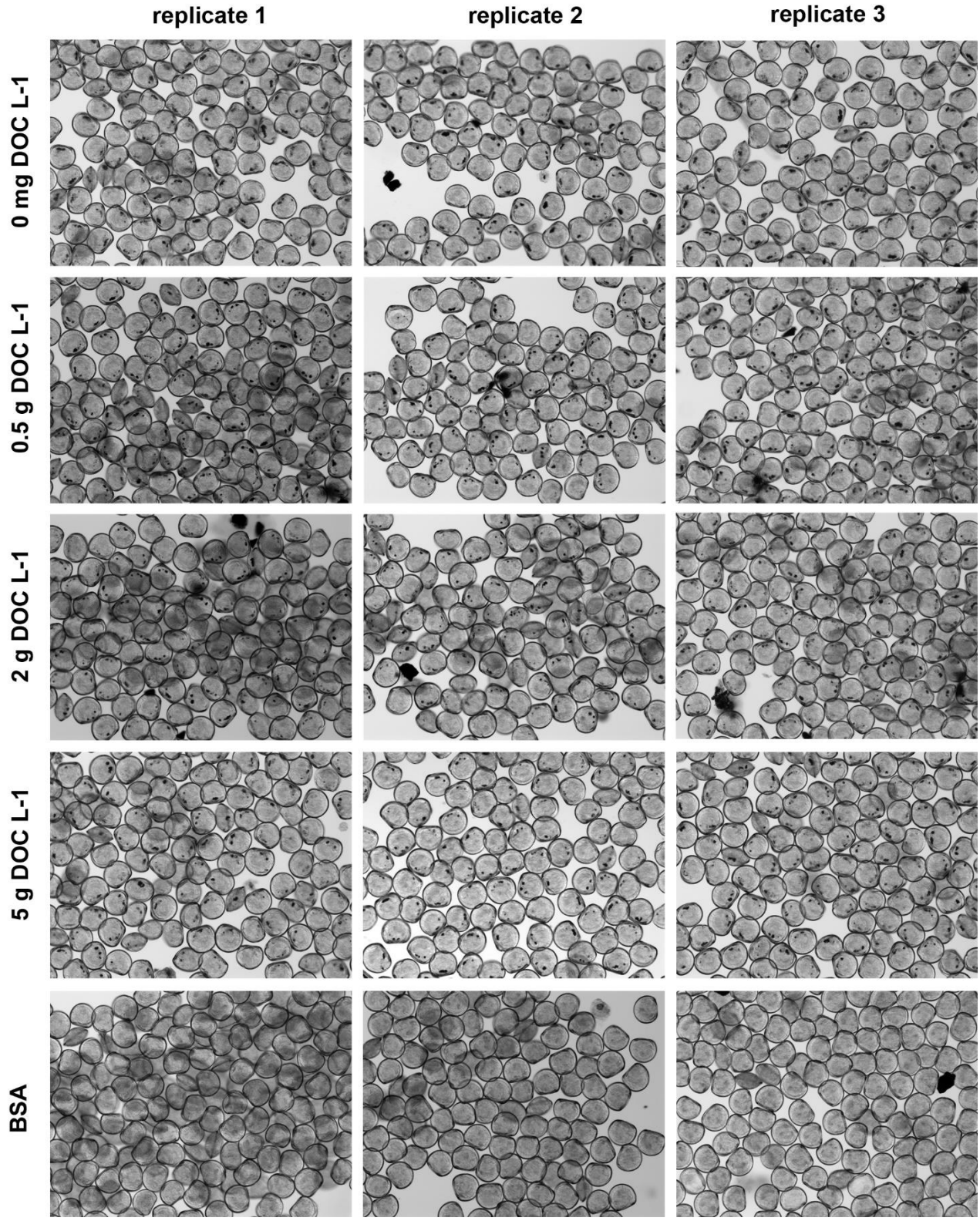

Figure S5. Ingestion of MnO_2 NPs by *C. gigas* larvae exposed for 48 h to 50 µM MnO_2 NPs. The black spots visible next to the shell's hinge are clumps of NPs in the digestive tract. Thus, they are indicative for active filtration and ingestion of NPs by oyster larvae.

Organisms exposed to the treatments containing 200 uM MnO_2 NPs

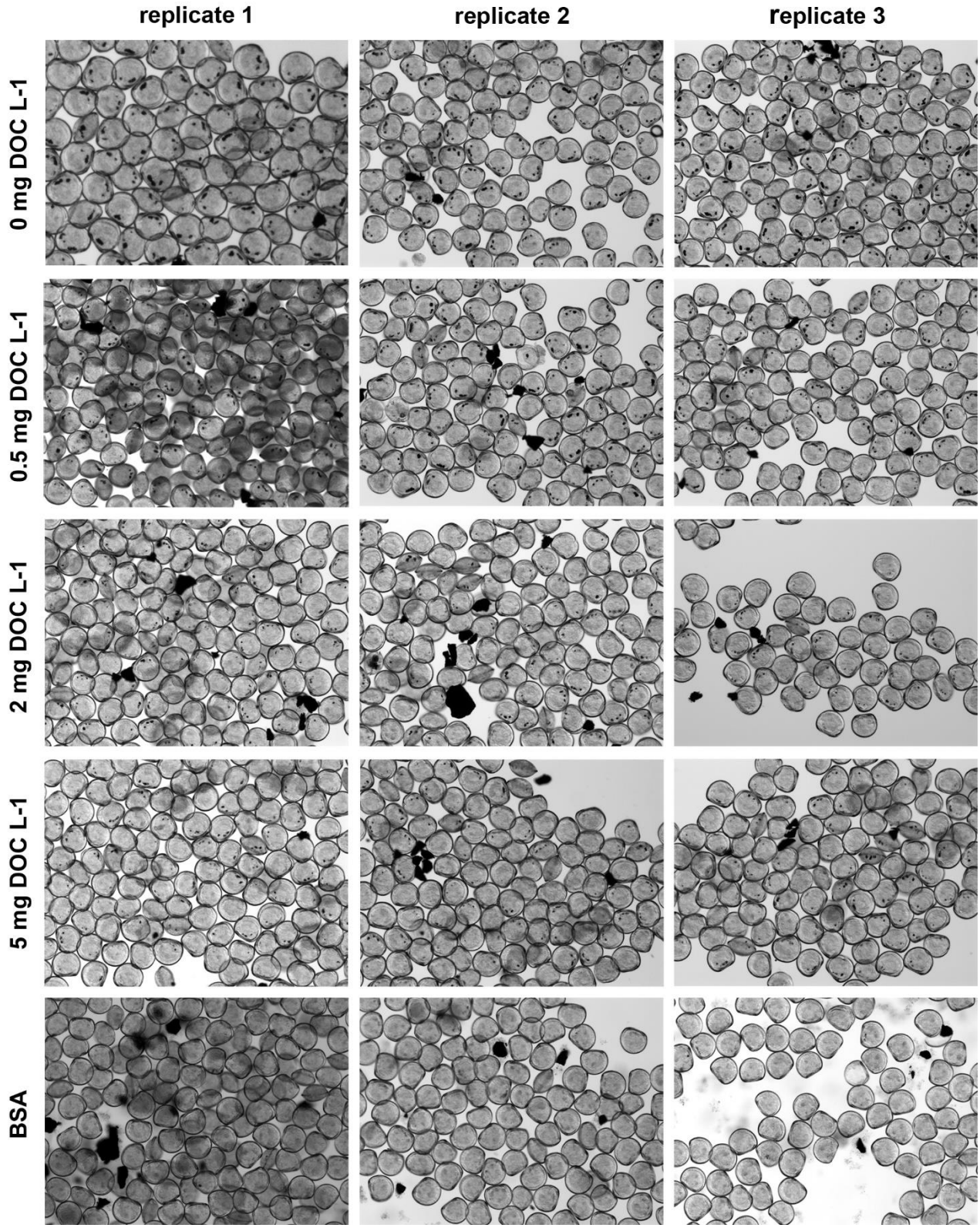

Figure S6. Ingestion of MnO_2 NPs by *C. gigas* larvae exposed for 48 h to 200 µM MnO_2 NPs. The black spots visible next to the shell's hinge are clumps of NPs in the digestive tract. Thus, they are indicative for active filtration and ingestion of NPs by oyster larvae.

TEM-EDS study of cellular internalization of MnO_2 NPs

Figure S7 and Table S4 present the results of the TEM-EDS analysis carried out to characterize the electron dense particle shown in Figure 4 (manuscript), and suspected to be a cellular internalized MnO_2 NP.

The high relative percentage of Mn over O (within the range characterizing the MnO_2 NP aggregates ingested by larvae and accumulated in the digestive tract) identified the suspected electron dense particle as a cellular internalized MnO_2 NP.

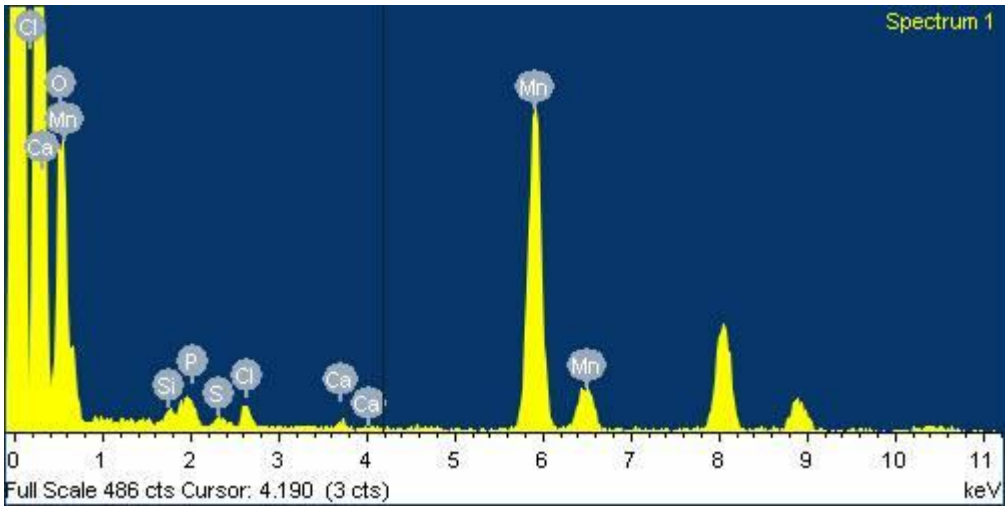

Figure S7. EDS spectra of Figure 4 (manuscript).

Table S4. Relative content of Mn and O recorded for the internalized MnO_2 NP (TEM-EDS). The relative percentage of Mn and O are also provided for reference elements (i.e. tissue areas bare of NnO_2 NPs, MnO_2 NPs).

		Mn %	O %
Suspicious electron dense particles analysed via TEM-EDS	Particle displayed in Figure 4 (manuscript)	21	79
References	**Tissue (larval tissue clear from MnO_2 NPs)**	**0**	**100**
	MnO_2 NPs	**14-26**	**86-74**

TEM-EDS analyses of electron dense particles suspected of being cellular internalized BSA coated MnO_2 NPs

TEM-EDS analysis was carried out to assess the chemical nature of some elements suspected to be ingested/cellular internalized BSA-coated MnO_2 NPs, because of their size/shape and electron density. Figure S8 present the electron dense particles characterized via TEM-EDS, and Table S5 reports their relative percentages of Mn and O, that were used to discriminate MnO_2 NPs from false positive.

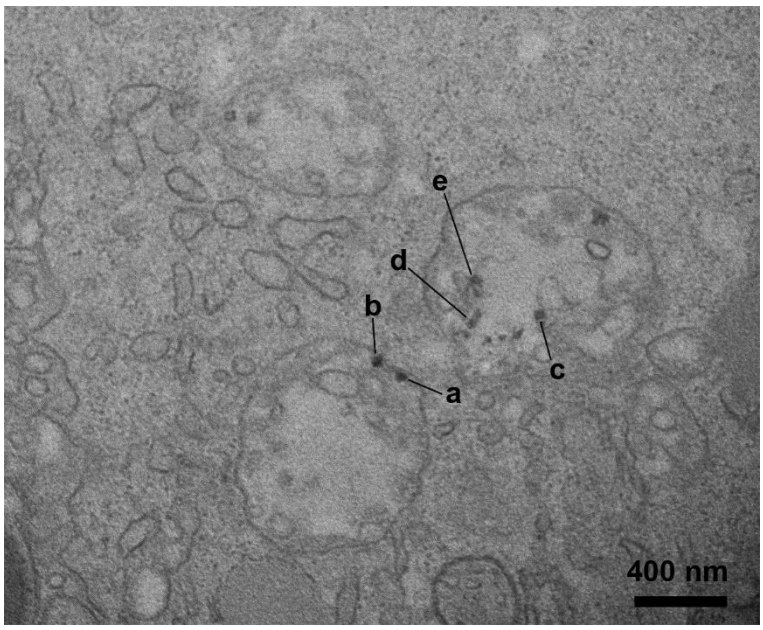

Figure S8. Suspicious electron dense particles (a-e) analysed for their chemical composition via TEM-EDS.

Table S5. Relative Mn and O content of the TEM-EDS analysed particles and reference elements (i.e. tissue areas bare of NnO2 NPs, cellular internalized NnO2 NPs).

		Mn %	O %
Suspicious electron dense particles analysed via TEM-EDS	Particle a	-1	101
	Particle b	0	100
	Particle c	-3	103
	Particle d	0	100
	Particle e	1	99
References	**Tissue (larval tissue clear from MnO_2 NPs)**	**0**	**100**
	Cellular internalised MnO_2 NPs (Figures 4 and S7)	**21**	**79**

References

1. JRC64075, NM-Series of Representative Manufactured Nanomaterials - Zinc Oxide NM-110, NM-111, NM-112, NM-113: Characterisation and Test Item Preparation.*Journal*, 2011, **http://publications.jrc.ec.europa.eu/repository/handle/JRC64075**.
2. C. H. Kim, Z. Akase, L. C. Zhang, A. H. Heuer, A. E. Newman and P. J. Hughes, The structure and ordering of epsilon-MnO2, *Journal of Solid State Chemistry*, 2006, **179**, 753-774.
3. H. Mai, P. Gonzalez, P. Pardon, N. Tapie, H. Budzinski, J. Cachot and B. Morin, Comparative responses of sperm cells and embryos of Pacific oyster (Crassostrea gigas) to exposure to metolachlor and its degradation products, *Aquatic Toxicology*, 2014, **147**, 48-56.
4. Y. Zhang, J. Li, F. Yu, X. C. He and Z. N. Yu, Allograft inflammatory factor-1 stimulates hemocyte immune activation by enhancing phagocytosis and expression of inflammatory cytokines in Crassostrea gigas, *Fish & Shellfish Immunology*, 2013, **34**, 1071-1077.
5. L. Zhang, L. Li and G. Zhang, Gene discovery, comparative analysis and expression profile reveal the complexity of the Crassostrea gigas apoptosis system, *Developmental & Comparative Immunology*, 2011, **35**, 603-610.
6. S. Vogeler, T. P. Bean, B. P. Lyons and T. S. Galloway, Dynamics of nuclear receptor gene expression during Pacific oyster development, *BMC Developmental Biology*, 2016, **16**, 33.